NASA

Technical Memorandum 82145

Cooling of Young Neutron Stars and The Einstein X-Ray Observations

Ken'ichi Nomoto and Sachiko Tsuruta

JUNE 1981

National Aeronautics and
Space Administration

Goddard Space Flight Center
Greenbelt, Maryland 20771

COOLING OF YOUNG NEUTRON STARS

AND

THE EINSTEIN X-RAY OBSERVATIONS

Ken'ichi Nomoto[1]

Laboratory for Astronomy and Solar Physics

NASA-Goddard Space Flight Center

and

Sachiko Tsuruta

Department of Physics, Montana State University

Received: _____

[1] On leave from Department of Physics, Ibaraki University, Japan

ABSTRACT

Cooling of neutron stars is calculated using an exact stellar evolution code. The full general relativistic version of the stellar structure equations are solved, with the best physical input currently available. For neutron stars with a stiff equation of state, we find that the deviation from the isothermality in the interior is significant and that it takes at least a few thousand years to reach the isothermal state. By comparing the most recent theoretical and observational results, we conclude that for Cas A, SN1006, and probably Tycho, "standard" cooling is inconsistent with the results from the Einstein Observatory, if neutron stars are assumed to be present in these objects. On the other hand, the "detection" points for RCW103 and the Crab are consistent with these theoretical results.

Subject headings : stars : neutron -- stars : interior --
nebulae : supernova remnant -- X-rays : sources.

I. INTRODUCTION

Until recently, the problem of neutron star cooling has been mainly of academic interest. Indeed, the sole information on the direct observation of surface radiation from neutron stars has been the upper limit for the Crab (Toor and Seward 1977). The exciting results from the Einstein Observatory are already changing the whole picture. As of March 1981, we have at least eight upper limits (Helfand 1981; Murray 1981; Pye et al. 1981; Seward 1981) and nearly a dozen possible "detections" (Harnden 1981; Helfand 1981; Tuohy and Garmire 1980) which may be related to neutron stars in young supernova remnants less than $\sim 10^5$yrs old. Prompted by these recent observational developments, we have re-examined theories of neutron star cooling. The most important factor which has been neglected in most of the earlier calculations is the effect of the finite timescale of thermal conduction.

In these calculations (Glen and Sutherland 1980; Tsuruta 1979; Van Riper and Lamb 1981), it was assumed that the central core is isothermal and that the thin outer envelope has constant photon luminosity. Under these assumptions, the surface temperature instantaneously follows the decrease in the central temperature through the escaping neutrinos. However, such a treatment is valid only if the timescale of thermal conduction is infinitely short as compared with the timescale of evolution. In the early stages of neutron star cooling, neutrino emission is much faster than thermal conduction, so that the thermal behavior of the surface layers does not necessarily keep pace with the neutrino

cooling in the interior. It has been shown that this effect is negligible for models with soft equations of state with age $t > \sim 10$ yrs (Malone 1974; Richardson 1980). Ray (1981) suggested through analytic estimates that, for some stiff equation of state stars with a large crust, this effect may be important because such a crust has a smaller conductivity and contains a significant fraction of the stellar mass. This question can be accurately answered by solving the equations of stellar structure simultaneously as a mixed initial-boundary-value problem. We have made such calculations for "standard" cooling of the stiff model by using an exact stellar evolution code. (By "standard" cooling we mean, following earlier convention, cooling in the absence of such exotic particles as pion condensates and quarks.) We have also recalculated the soft model using the isothermal method, because we are currently interested only in stars older than $\sim$ 100 yrs. In both cases, we have made use of the best theoretical knowledge currently available. In this Letter, we briefly report our results with particular emphasis on the stiff model and compare them with observational data. A more detailed description and discussion will be given elsewhere.

II. PHYSICAL INPUT

Physical input for the exact evolution calculation is the following: The full general relativistic equations (Thorne 1977) are adopted for the hydrostatic equilibrium, thermal energy transport, and energy conservation. These equations are integrated simultaneously as a function

of time and space coordinates by using a Henyey-type stellar evolution code (Sugimoto 1970). We use a stiff equation of state by Pandharipande, Pines, and Smith (1976) generally called the PS model, based on tensor interactions between nucleons, for $\rho > 4.3 \times 10^{11}$g cm^{-3}, and the finite temperature equation of state for a mixture of electrons and ions for $\rho \leq 4.3 \times 10^{11}$g cm^{-3}. ($\rho$ denotes the matter density.) The density at the boundary of the heavy ion crust and the central nucleon liquid core is chosen to be 2.2×10^{14}g cm^{-3}. Specific heats of all fermions (neutrons, protons and electrons) and heavy ions are included and the effects of crystalization are taken into account. Neutrino emissivities included are: modified URCA, neutron-neutron and neutron-proton bremsstrahlung (Friman and Maxwell 1979), electron-ion bremsstrahlung (Soyeur and Brown 1979), and plasmon, pair and photo neutrino emissivisites (Beaudet et al. 1967). Weinberg-Salam theory with the Weinberg angle $\sin^2\theta_W = 0.23$ is applied. Electron, muon and tau neutrinos are included.

We adopt the approach of Maxwell (1979) in taking into account the effect of superfluid protons and neutrons on neutrino emissivities and specific heats. The critical temperatures, $T_{cr}^{(n)}$ and $T_{cr}^{(p)}$, for superfluid neutrons and protons are given by Takatsuka (1972) and Chao et al. (1972), respectively. We set the effective mass $m_n^*/m_n = m_p^*/m_p = 0.8$. We use the Los Alamos table (Huebnar et al. 1977) for iron radiative opacities and work by Flowers and Itoh (1976, 1979) for conductive opacities. The effect of magnetic fields on opacities is taken into account by adopting the approach of Tsuruta (1979).

III. RESULTS

Our results are summarized in Figures 1 and 2, for the PS model where: the gravitational mass is $M_G = 1.31\ M_\odot$ (the rest mass $M_A = 1.40 M_\odot$), the stellar radius is R = 16.1 km (the "apparent" radius $R^\infty = 18.5$ km), the central density is $\rho_c = 4.0 \times 10^{14}$ g cm^{-3}, the redshift correction factors (Thorne 1977) are $e^\phi = 0.75$ and 0.87 at the center and at the surface, respectively (ϕ is the gravitational potential), the mass of the central nucleon core is $0.8\ M_\odot$, and the thickness of the crust is 5.4 km.

In Figure 1, the "standard" cooling curves are shown for four cases: Case S with superfluid nucleons and Case N with non-superfluid (normal) nucleons both for the zero magnetic field, and Cases MS (superfluid) and MN (non-superfluid) for the magnetic field of $H = 4.4 \times 10^{12}$ gauss. In Figure 2, the evolutionary change in the local temperature distribution is shown as a function of local density for Cases S and N. (The stages with the same number, #0 - 8, correspond to the same age.) The effects of the finite timescale of thermal conduction are clearly seen in these figures. The important outcome is that (i) the temperature distribution in the interior deviates significantly from the isothermality for as long as a few thousand years, and that (ii) unlike the smooth fall which is the characteristic of the isothermal cases, the surface temperature T_e^∞ declines as follows.

a) Superfluid Neutron Stars (Case S)

Phase I ($t \lesssim 10^{-2}$yrs): The initial (#0) model with the central temperature $T_c = 1 \times 10^{10}$K was constructed by suppressing neutrino emission and choosing a long enough time step to reach the thermally relaxed state. Afterwards, neutrino emission is turned on. The neutrino energy loss rate, ε_ν, dominates over the photon cooling rate, $\varepsilon_{ph} \equiv e^{-2\phi} \partial(e^{2\phi}L_r)/\partial M_r$ (i.e., $\varepsilon_\nu >> |\varepsilon_{ph}|$) in the interior where $\rho > \sim 10^9$g cm^{-3}. On the other hand, $\varepsilon_{ph} > \varepsilon_\nu$ in the surface layers. In Figure 2, the line for $\varepsilon_\nu = \varepsilon_{ph}$ is shown for several stages.

The nucleon core ($\rho > 2 \times 10^{14}$g cm^{-3}) is cooled by the modified URCA neutrino emission. The neutrons in the region 10^{13}g cm$^{-3} \lesssim \rho \lesssim 10^{14}$ g cm^{-3} become $^1S_0$ superfluid. (The corresponding maximum superfluid critical temperature in this region is $T_{cr}^{(n)} \sim 1.7 \times 10^{10}$K.) The greatly decreased specific heat at $T << T_{cr}^{(n)}$ causes the valley in this region (Figure 2, #1). The trough around $\rho \sim 10^{11}$g cm^{-3} is due to the plasmon neutrino losses; the density dependence of ε_ν causes the temperature inversion at $\rho \sim 10^9$-10^{11}g cm^{-3}. As a result, the temperature peak appears near $\rho \sim 10^9$-10^{10}g cm^{-3}(#1).

The central temperature T_c decreases monotonically during this phase, but the temperature near the surface ($\rho < \sim 10^9$g cm^{-3}) stays almost constant, because a period of $\sim 10^{-2}$yrs is too short for thermal conduction to be effective.

Phase II ($10^{-2} < t \lesssim 1$ yr): This phase is characterized by the appreciable decline of T_e^∞ as seen in Figure 1 (##1 - 3). This decline

is caused by the decrease of the temperature peak around the outer crust of $\rho \approx \sim 10^9$-10^{10} g cm^{-3} through the plasmon neutrino emission. Since photon cooling is dominant ($\varepsilon_{ph} > \varepsilon_\nu$) in the surface layers where $\rho < \sim 10^9$ g cm^{-3}, T_e^∞ decreases simultaneously with the temperature fall of this boundary region. By the end of this phase, the central dips in Figure 2 disappear because the URCA process begins to be suppressed by the proton superfluidity at $T \sim T_{cr}^{(p)} \sim 6 \times 10^8$ K.

Phase III (1 yr < t $\lesssim$ 20 yrs): The decreases in T_e^∞ turn out to be very slow (##3 - 4) as compared with Phase II. Neither thermal conduction nor the plasmon neutrino emission in the outer crust are effective in cooling the surface layers. Thermal conduction is not efficient enough to make the interior isothermal; the temperature in the central nucleon core is higher than in the crust because of the suppression of the URCA process.

Phase IV (20 yrs < t $\lesssim$ 400 yrs): T_e^∞ decreases significantly again (##4 - 6). The thermal conduction timescale starts becoming comparable with the cooling rate due mainly to the crust neutrino bremsstrahlung in the inner crust. Accordingly, this neutrino cooling is effectively transmitted to the surface. The temperature in the nucleon core, however, is still appreciably higher than the crust temperature.

Phase V (400 < t $\lesssim$ 4000 yrs): The neutron star approaches a thermally relaxed state (##6 - 7), while appreciable heat flow occurs from the hotter core to the cooler crust layers. At t $\sim$ 4000 yrs, the isothermal state is almost reached.

Phase VI (4000 yrs < t): The cooling is now so slow that the isothermal approximation is valid.

b) Non-Superfluid Neutron Star (Case N)

As shown in Figure 2, the cooling in the central nucleon core is much faster than in Case S because the URCA process is not suppressed by the proton superfluidity. The inner crust layers are hotter than in Case S because the neutron specific heat is not suppressed by the $^1S_0$ superfluidity. The cooling curve in the earlier stages, which is controlled by the plasmon neutrino emission in the outer layers, is identical to Case S until $t \simeq 20$ yrs (until the end of Phase III). During Phase IV, T_e^∞ in Case N is higher than in Case S because of the higher temperatures in the inner crust layers. Later in Phase V, T_e^∞ is lower than in Case S due to the effect of the faster URCA cooling in the core. Contrary to Case S, heat flows inward from the hotter crust to the cooler core during the stages approaching the thermal relaxation (Figure 2). In Case N, the isothermal state is reached at $t \sim 1500$ yrs.

c) Magnetic Neutron Star (Cases MS and MN)

The interior evolution for cases MS (superfluid) and MN (non-superfluid) are similar to the corresponding zero-field cases S and N. The effects of the reduced opacity near the surface under the strong magnetic fields begin to be significant at $t \simeq 1$ yr. Afterwards the cooling is slower than the zero field cases, except that the final declines of T_e^∞ are steeper when photon emission overtakes neutrino emissions as the main cooling agent ($t \gtrsim 5 \times 10^4$yrs).

d) Other Cases

Similar calculations have been carried out for the PS model with 0.4 $M_\odot$ and 0.8 $M_\odot$, and qualitatively similar results are obtained.

By using the same physical input, we updated the earlier calculations (Tsuruta 1980) for the soft model (the BPS model; Baym et al. 1971); M_G = 1.3 $M_\odot$ and R = 8.0 km (R^∞ = 11 km). We used the isothermal approximation, which is valid for stars older than at least $\sim$ 100 yrs (see §I). Our new results for the BPS model (see Figure 3) are essentially the same as those reported earlier (Tsuruta 1980).

IV. COMPARISON WITH OBSERVATION AND DISCUSSION

In Figure 3, the preceding theoretical results are compared with observational data. The solid curves refer to models which include superfluidity, while the dashed curves correspond to those with no superfluid particles. The upper curves represent strongly magnetized stars with H = 4.4 x 10^{12}gauss, while the lower curves are for the zero field case. The stellar mass is 1.3 $M_\odot$, which is consistent with both current theory and observation. The crosses indicate the observed upper limits to the surface temperatures of various young supernova remnants assuming the presence of neutron stars in these objects (Murray 1981; Fabbiano 1981; Seward 1981; Helfand 1981). The circles refer to possible "detection" of point sources (Harnden 1981; Tuohy and Garmire 1980). These points are accompanied by the estimated error bars which

are mostly due to the uncertainty in the interstellar absorption. (Strictly speaking, the Crab "detection" should still be regarded as an "upper limit". However, it should be distinguished from the other upper limits, because unpulsed soft X-rays were indeed detected from the Crab pulsar while the upper limits in the other cases were determined by the non-detection of point sources (Harnden 1981).)

We note:

(i) Some of the observed upper limits, for Cas A, SN1006, and probably Tycho, are below the "standard" theoretical curves. A natural interpretation is that there are no neutron stars in these supernova remnants (Tsuruta 1980), or that these stars contain such exotic particles as charged pion condensates (Tsuruta 1979) and quarks (Iwamoto 1980; Van Riper and Lamb 1981). Since Tycho is thought to be a remnant of Type I Supernova (SN I), the present result is consistent with the detonation/deflagration-type explosion model for SN I which disrupts the star completely and leaves no neutron star (see Nomoto 1980 for a review).

(ii) The "detection" points for RCW103 and the Crab are consistent with these "standard" theoretical curves.

The "detection" point for Vela is still preliminary (Harnden 1981). Very recently, possible "detection" of point sources has been reported for several other supernova remnants, e.g., 3C58 and CTB80 (Becker, Helfand, and Szymkowiak 1981; Helfand 1981). Further careful investigation is required, however, before we can properly interprete the observational data for these sources.

We note that our curves for the PS model are significantly higher

than those of Van Riper and Lamb (1981), while they are somewhat lower than those by Glen and Sutherland (1980). For instance, for Case S at t = 1000 yrs, our photon luminosity L_{ph}^{∞} is $\sim$ 6 times higher than that of Van Riper and Lamb, while it is a factor of $\sim$ 2 lower than that of Glen and Sutherland. It appears that the lower boundary of the BPS model by these three groups agree within the uncertainty inherent in the current theories of opacity and superfluidity. Our upper boundary for the BPS model in higher than those of the other two groups, because we included the possibility that protons may very well be in a state of p-wave superfluidity in a high density region where $\rho = \sim 10^{15} - 5 \times 10^{15}$g cm^{-3} (Tsuruta 1979). See Tsuruta (1981) for a more complete comparison of theoretical results of different groups. (We should remark here that in the comparison made above, we used the luminosity scale in Figure 3 of the Van Riper and Lamb (1981) paper, because their BPS temperature scale is in error.)

Van Riper and Lamb (1981) reached essentially the same conclusion as ours for SN1006 and Tycho. However, for the Crab and Cas A, the conclusion they present contradicts ours, as their observed points for these sources lie above their "standard" theoretical curves. The major reason for this is their misplacement of these observed points (Figure 3 of Van Riper and Lamb 1981).

V. CONCLUDING REMARKS

Our most significant finding is that for the stiff model the effects

of a finite timescale of thermal conduction are quite important. For the stiff PS model of mass 1.3 $M_\odot$, it takes $\sim$ 4000 yrs for Case S and $\sim$ 1500 yrs for Case N, before the isothermal state is reached.

Many young supernova remnants (Cas A, Kepler, Tycho, Crab, RCW103, and W28) have an age of a few thousand yrs or less. Therefore, for the stiff model, it appears that the earlier cooling calculations using an isothermal approximation are inadequate and we have to resort to exact stellar evolution calculations such as those presented here, if we are to make relevant quantitative comparisons between theory and the greatly improved observational data now available from the Einstein Observatory and those expected from the observational programs planned for the near future.

We wish to thank Drs. G. Fabbiano, F.R. Harnden, D.J. Helfand, S.S. Murray and F.D. Seward, for the carefully checked observational information, and W. Huebner for the opacity table. We would also like to thank Professor D. Sugimoto for his suggestion of the importance of this work, Drs. T. Murai and N. Itoh for their contribution in the initial stage of our investigation (Nomoto et al. 1980), and H. Nomoto for preparation of the manuscript. ST is particularly grateful to Professors R. Giacconi and R.J. Swenson, among the many of her colleagues who have given her encouragement and help. KN is grateful to Dr. W.M. Sparks for encouragement. This work is partly supported by the NRC-NASA Research Associateship in 1979-1981.

REFERENCES

Baym, G., Pethick, C.J., and Sutherland, P.G. 1971, Ap.J., 170, 299.

Beaudet, G., Petrosian, V., and Salpeter, E.E. 1967, Ap.J., 150, 979.

Becker, R.H., Helfand, D.J., and Szymkowiak, A.E. 1981, B.A.P.S., 26, 570.

Chao, N.-C., Clark, J.W., and Yang, C.H. 1972, Nucl. Phys., A179, 320.

Fabbiano, G. 1981, private communication.

Flowers, E.G. and Itoh, N. 1976, Ap.J., 206, 218.

Flowers, E.G. and Itoh, N. 1979, Ap.J., 230, 847.

Friman, B.L. and Maxwell, O.V. 1979, Ap.J., 232, 541.

Glen, G. and Sutherland, P.G. 1980, Ap.J., 239, 671.

Harnden, F.R. 1981, private communication.

Helfand, D.J. 1981, private communication; also in IAU Symposium No.95, Pulsars, ed. R. Wielebinski and W. Sieber (Dordrecht: Reidel), in press.

Huebner, W.F., Merts, A.L., Magee, N.H. Jr., and Argo, M.F. 1977, Los Alamos National Laboratory report LA-6760-M.

Iwamoto, N. 1980, Phys. Rev. Letters, 44, 1637.

Malone, R.C. 1974, Ph.D. Thesis, Cornell University.

Maxwell, O.V. 1979, Ap.J., 231, 201.

Murray, S.S. 1981, private communication.

Nomoto, K. 1980, in IAU Symposium No.93, Fundamental Problems in the Theory of Stellar Evolution, ed. D. Sugimoto, D.Q. Lamb, and D.N. Schramm (Dordrecht: Reidel), in press.

Nomoto, K., Tsuruta, S., Murai, T., and Itoh, N. 1980, in Proc. Symposium on Space Astrophysics, ed. S. Hayakawa (Tokyo: ISAS, Univ. of Tokyo), p. 210.

Pandharipande, V.R., Pines, D., and Smith, R.A. 1976, Ap.J., 208, 550.

Pye, J.P., Pounds, K.A., Rolf, D.P., Seward, F.D., Smith, A., and Willingale, R. 1981, M.N.R.A.S., 194, 569.

Ray, A. 1981, Nucl. Phys., A356, 523.

Richardson, M.B. 1980, Ph.D. Thesis, State University of New York at Albany.

Seward, F.D. 1981, private communication.

Soyeur, M. and Brown, G.E. 1979, Nucl. Phys., A324, 464.

Sugimoto, D. 1970, Ap.J., 159, 619.

Takatsuka, T. 1972, Prog. Theor. Phys., 48, 1517.

Thorne, K.S. 1977, Ap.J., 212, 825.

Toor, A. and Seward, F.J. 1977, Ap.J., 216, 560.

Tsuruta, S. 1979, Phys. Rept., 56, 237.

Tsuruta, S. 1980, in X-Ray Astronomy, ed. R. Giacconi and G. Setti (Dordrecht: Reidel), p.73; also in IAU Symposium No.95, Pulsars, ed. R. Wielebinski and W. Sieber (Dordrecht: Reidel), in press.

Tsuruta, S. 1981, to appear in Comments on Astrophysics, Review Section.

Tuohy, I. and Garmire, G. 1980, Ap.J. Letters, 239, L107.

Van Riper, K.A. and Lamb, D.Q. 1981, Ap.J. Letters, 244, L13.

FIGURE CAPTIONS

Figure 1: The surface temperature T_e^∞ and photon luminosity L_{ph}^∞ (both observed at infinity) are shown as a function of age (measured at infinity) for the PS model with $M_G = 1.3\ M_\odot$.

Figure 2: Distribution of local internal temperature as a function of local matter density at different evolutionary stages ##0 - 8 for the PS model with $M_G = 1.3\ M_\odot$ and H = 0. Nucleon superfluidities are included in Case S (upper half), while they are absent in Case N (lower half).

Figure 3: Comparison between the observational results from the Einstein Observatory and the theoretical curves for "standard" cooling of the PS model (upper half) and the BPS model (lower half). T_e^∞ (left) and I_{ph}° (right) are shown as a function of age (measured at infinity). The numbers refer to the observational data of: (1) Cas A, (2) Kepler, (3) Tycho, (4) Crab, (5) SN1006, (6) RCW103, (7) RCW86, (8) W28, (9) G350.0 - 18 , and (10) G22.7 - 0.2.

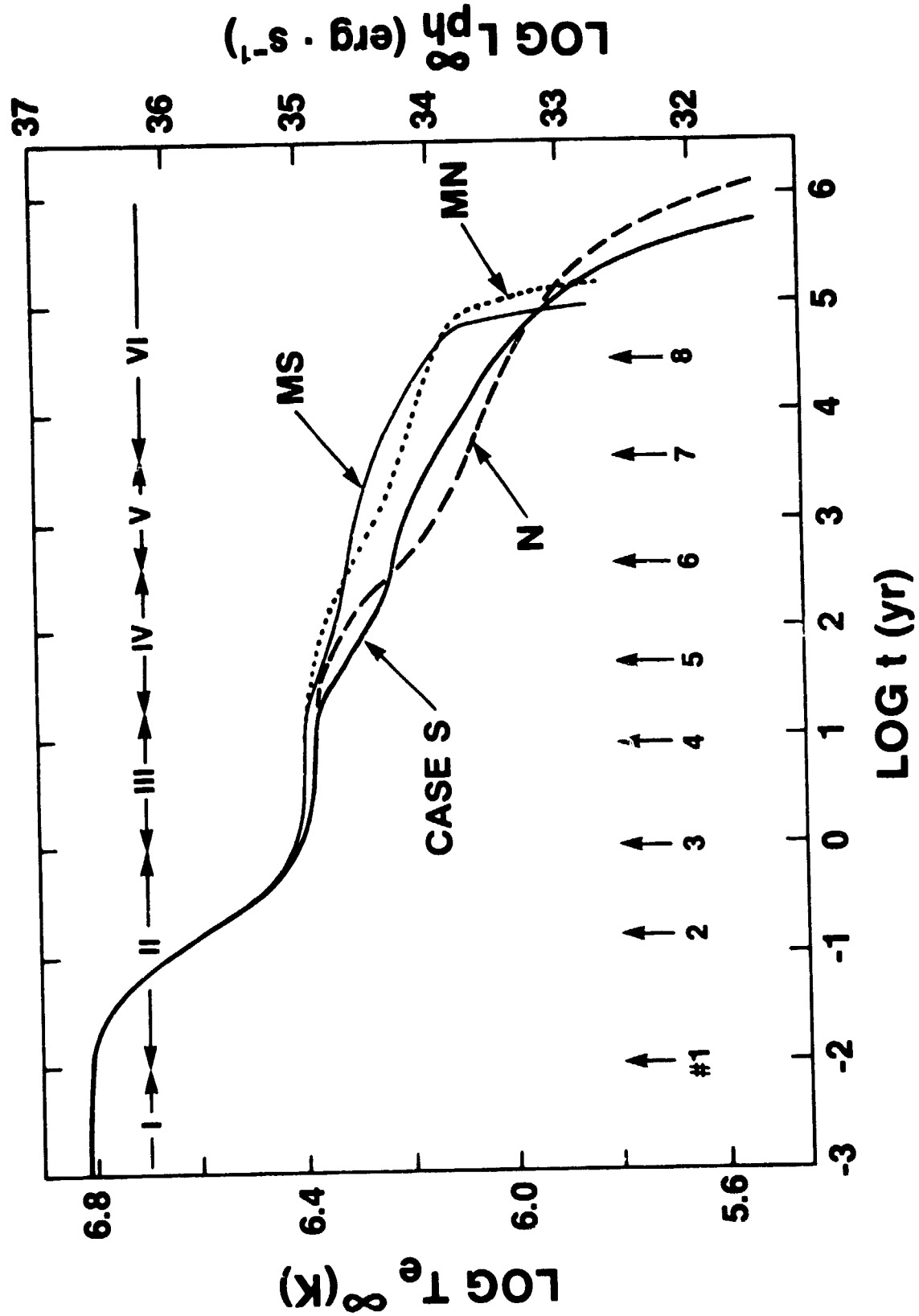
LOG L_{ph}^{8} (erg · s^{-1})
37
36
35
34
33
32
MN
MS
N
CASE S
I
II
III
IV
V
VI
#1
2
3
4
5
6
7
8
6
5
4
3
2
1
0
-1
-2
-3
LOG t (yr)
LOG T_e ^{8}(K)
6.8
6.4
6.0
5.6

Figure 1.

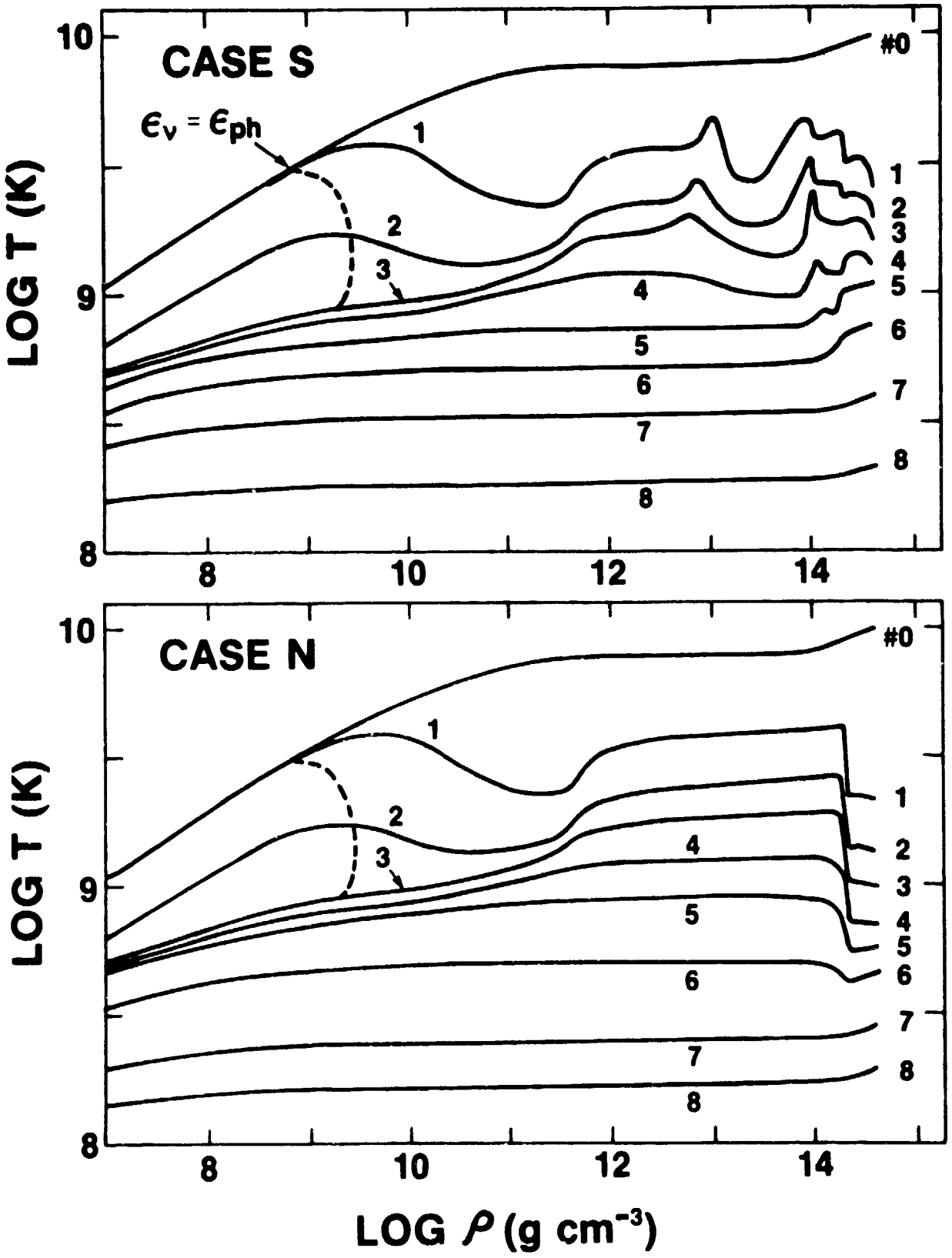
CASE S
$\epsilon_\nu = \epsilon_{ph}$
#0
1
2
3
4
5
6
7
8
LOG T (K)
10
9
8
8
10
12
14
CASE N
LOG ρ (g cm^{-3})

Figure 2.

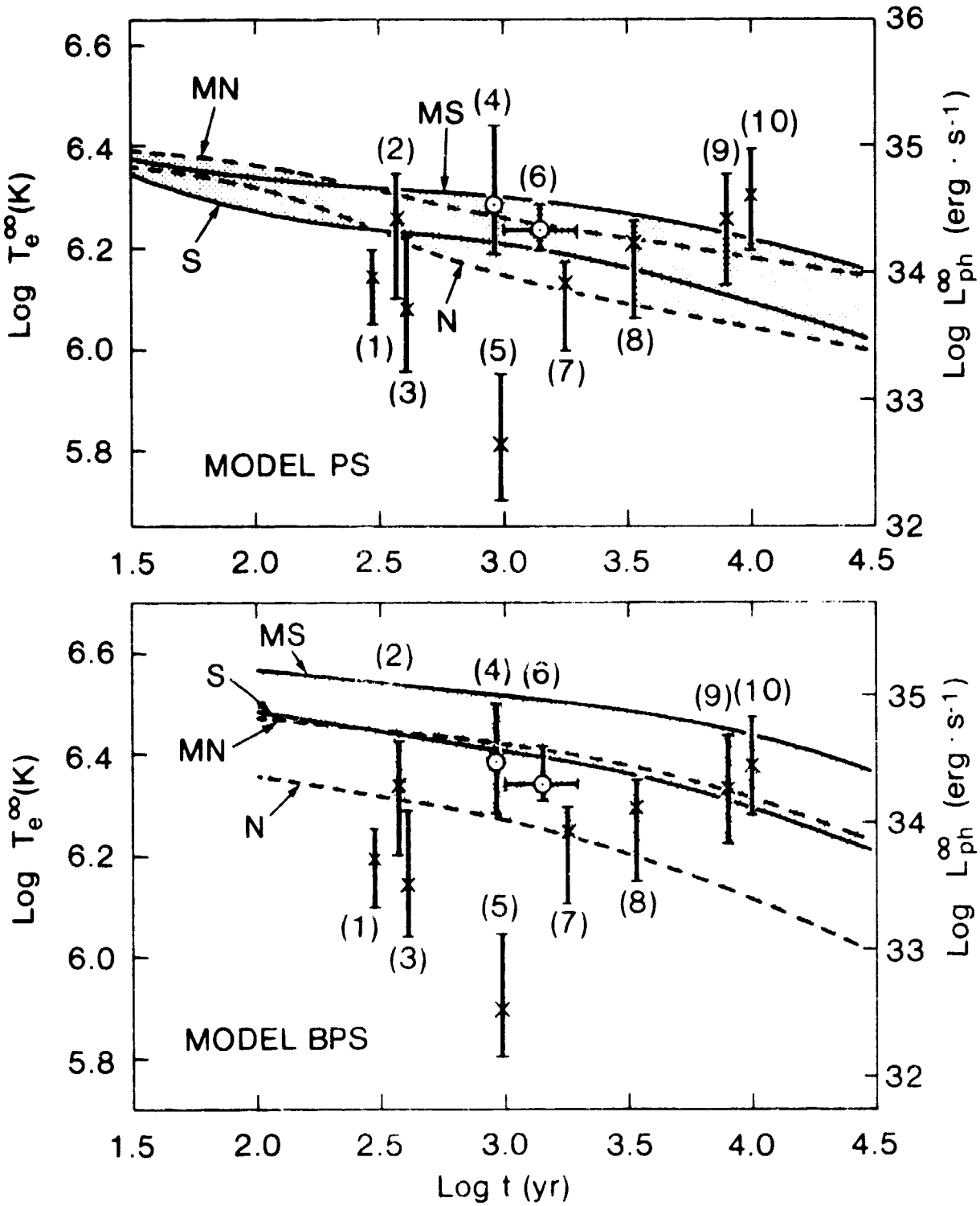
MODEL PS
MODEL BPS
MN
MS
S
N
(1)
(2)
(3)
(4)
(5)
(6)
(7)
(8)
(9)
(10)
Log T_e^∞(K)
Log L_{ph}^∞ (erg · s^{-1})
Log t (yr)
6.6
6.4
6.2
6.0
5.8
36
35
34
33
32
1.5
2.0
2.5
3.0
3.5
4.0
4.5

Figure 3.